Identification of the Jet-Cooled 1-Indanyl Radical by Electronic Spectroscopy

Tyler P. Troy, Masakazu Nakajima, Nahid Chalyavi, Raphaël G. C. R. Clady, Klaas Nauta, Scott H. Kable, and Timothy W. Schmidt*

School of Chemistry, University of Sydney, NSW 2006, Australia

Received: June 22, 2009; Revised Manuscript Received: August 10, 2009

The electronic spectrum of the jet-cooled 1-indanyl radical has been identified in the products of a hydrocarbon discharge in argon. Electronic excitation spectra were observed in the region 20800−22600 cm^{-1} by resonant two-color two-photon ionization and laser-induced fluorescence spectroscopies. In addition to the new spectrum at $m/z = 117$, the spectrum of 1-phenylpropargyl was also observed strongly, as was an unidentified spectrum carried by $m/z = 133$. The origin band of the 1-indanyl $\tilde{A}^2A''-\tilde{X}^2A''$ band system was observed at 21159 cm^{-1} with the ionization potential of the radical experimentally determined to be 6.578 ± 0.001 eV from a photoionization efficiency spectrum. Single vibronic level fluorescence was dispersed to determine the ground state vibrational frequencies that were utilized to confirm the identity of the radical in comparison with quantum chemical calculations. The calculated ground state frequencies and ionization potential, along with a calculated dispersed fluorescence spectrum of the origin band for the 1-indanyl radical, all provide a positive chemical identification.

Introduction

Resonance stabilized radicals (RSRs) are of considerable interest owing to their proposed role in the formation of benzene and subsequently polycyclic aromatic hydrocarbons (PAHs).[1,2] Because of the delocalization of the unpaired electron, the stabilization of RSRs results in slower reaction rates compared with localized radicals such as phenyl or methyl. They have also been found to be preferentially formed following the decomposition of stable molecules and exhibit slower rates of subsequent dissociation compared to localized radicals.[3−5] As a consequence, RSRs are able to reach higher concentrations in chemical reactions. This kinetic advantage is considered to allow the efficient formation of larger molecules through their reactions with themselves and with other RSRs. While the path to benzene is widely believed to follow propargyl self-reaction, the processes that lead to adjunct ring addition remain speculative.[6−11] As such, it is of interest to investigate RSRs that are possible intermediates connecting benzene and larger PAHs. Such polycyclics are considered to play a crucial role in soot formation from hydrocarbon combustion.

The chemistry involved in soot formation from combustion is also applicable to the chemistry of circumstellar and interstellar environments, which are generally considered to be rich in PAHs.[12] Generally, radical−radical recombination reactions are barrierless processes that can proceed in low temperature extraterrestrial conditions. RSR recombination therefore provides one mechanism for the formation of PAHs in space. Furthermore, radicals carrying the benzylic moiety are of special interest since they exhibit visible transitions that may prove related to the diffuse interstellar band (DIB) phenomena.[13] Combining these themes, the 1-indanyl radical (Figure 1) is a prototypical polycyclic aromatic RSR.

Indene (Figure 1) is observed to form following the discharge of either benzene or 1,3-butadiene in addition to the formation of other higher mass aromatics such as tolane, naphthalene, and fluorene.[14,15] In a computational study by Vereecken et al. of the addition of propyne to phenyl radical to yield indene as a PAH, the 1-indanyl radical was found to be the minimum on an extensive and comprehensive C_9H_9 potential energy surface.[10] Moreover, the formation of the resonance-stabilized 1-indanyl radical from indene and atomic hydrogen was found to be barrierless, indicating that indene-like moieties, more generally, could act as a sink of hydrogen atoms at low temperatures to yield the corresponding RSR. With its implied role in indene formation, and its calculated high stability, it is of interest to identify its spectrum as an isolated (in vacuo) radical.

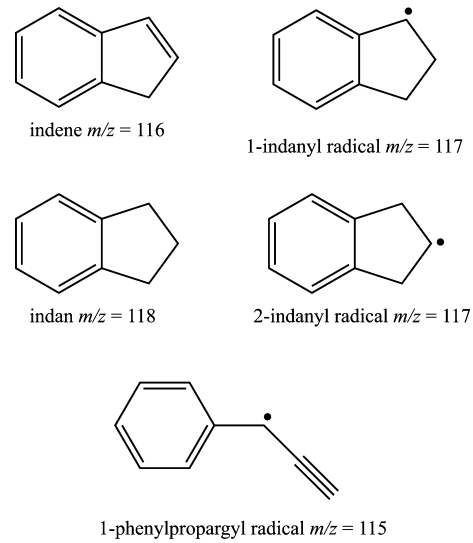

Figure 1. Structures of molecules and radicals in this work.

The blue fluorescence induced by an electrical discharge in indene and indan vapor was first observed by McVicker et al. in the 1920s.[16] Subsequent investigations observed the same emission from γ-irradiated indene and indan samples trapped in glassy matrices.[17−19] This emission was assigned to the 1-indanyl radical assuming respective gain or loss of an

* To whom correspondence should be addressed. E-mail: t.schmidt@chem.usyd.edu.au.

10.1021/jp905831m CCC: $40.75
Published on Web 09/01/2009

α-hydrogen atom from the parent indene or indan. Hydrogen loss at the α-position is considered to be the most plausible outcome of γ-irradiation since similar experiments involving toluene and durene molecules were found to lead to the formation of benzyl and duryl radicals respectively.[17,20,21] Izumida et al. reported the excitation spectrum of the 1-indanyl radical observed from the γ-irradiation of indene in a glassy matrix.[19] The low resolution of these spectra and matrix effects have limited the assignment of the observed features, and a thorough argument for the 1-indanyl radical carrying the spectral bands is wanting. In this article, we report the laser-induced excitation and emission spectra of the 1-indanyl radical observed in the jet-cooled products of an electrical discharge of argon-containing indene. Quantum chemical calculations were performed to aid the unambiguous identification of the spectral carrier and to assist in the assignment of the observed vibrational structures.

Experimental Section

Laser-Induced Fluorescence (LIF) Spectroscopy. A pulsed discharge nozzle (PDN) was used to produce the species of interest. The vapor pressure of a precursor, indene (Fluka, 95%, 1.9 Torr at 300K) or indan (Aldrich, 95%) was seeded in argon (4 bar, 298 K) and expanded into a vacuum chamber. A voltage of −1.5 kV of 30 μs duration was applied to the outer electrode of the PDN through 2.5 kΩ ballast resistor, timed to strike during the gas expansion. A jet containing hydrocarbon radicals was interrogated ∼2 cm downstream by the output of a XeCl excimer laser pumped dye laser.

For measurements of excitation spectra, the induced fluorescence was imaged by a quartz lens onto the entrance slit of a 0.25 m monochromator mounted to the vacuum chamber at 90° to the laser beam. The monochromator, equipped with horizontal 5.0 mm entry and exit slits, was tuned to 500 nm and used as a bandpass filter to minimize scattered laser light and discharge afterglow. The fluorescence passed through the monochromator was detected by a photomultiplier tube (PMT). Spectra were corrected by measurement of the relative laser intensity with a photodiode. Absolute frequency calibration of the laser was achieved using a wavemeter.

A dispersed fluorescence (DF) spectrum was measured by fixing the pump laser frequency at the origin band (21159 cm^{-1}). A lens assembly was used to collimate and image the fluorescence onto the horizontally aligned entrance slit of a 0.75 m monochromator operated with slit-widths of 200 μm, corresponding to a spectral resolution of approximately 10 cm^{-1}. The monochromator was calibrated between 15 000 and 25 000 cm^{-1} with a sodium lamp, using known emission lines of sodium and argon. Reported emission frequencies are expected to be accurate to within 1 cm^{-1}. The fluorescence signal was digitized with a 500 MHz oscilloscope and transferred to a personal computer to be processed. Relative instrument timings were controlled by a digital delay generator operated at a repetition rate of 10 Hz.

Resonant Two-Color Two-Photon Ionization. Resonant two-color two-photon ionization (R2C2PI) spectra were measured in a two-stage differentially pumped vacuum chamber. A free jet containing hydrocarbon radicals was produced by a PDN as described above. The supersonically cooled jet was skimmed with a 2 mm skimmer and the resulting molecular beam was passed between the grids of a time-of-flight mass spectrometer. Radicals were cooperatively ionized by two laser pulses. Tunable radiation was provided by a XeCl excimer laser pumped dye laser. The ionization pulse, the 266 nm output from a Nd:YAG laser, was counter-propagated with the tunable laser beam. The positive ions were extracted vertically and perpendicular to the laser and molecular beam into the time-of-flight tube. The accelerating voltage was 2050 V, applied to the bottom extraction grid. Ions were detected with a tandem microchannel plate. Time-resolved ion signals were buffered by a digital oscilloscope and processed on a personal computer. Relative instrument timings were controlled by a digital delay generator operated at a repetition rate of 10 Hz. A photoionization efficiency curve of a carrier at $m/z = 117$ was obtained by scanning the frequency-doubled output of a Nd:YAG-pumped dye laser as the second, ionizing photon.

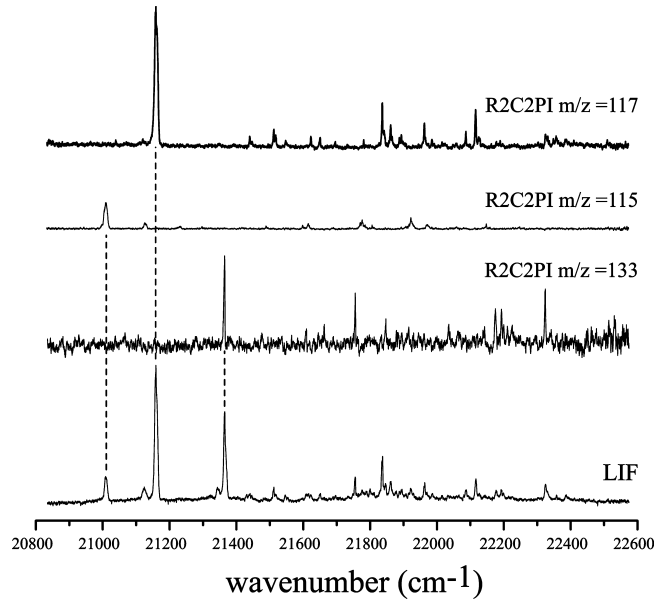

Figure 2. The excitation spectra of an indene/argon discharge in the indicated region recorded using LIF and R2C2PI. The features of the LIF spectrum were accounted for by resonant ionization spectra collected on $m/z = 115$ (1-phenylpropargyl),[11] $m/z = 117$ (1-indanyl, see text) and $m/z = 133$ (unidentified). The principal band positions observed for the $m/z = 117$ carrier are 21159, 21836, 22115, and 22327 cm^{-1}.

Results and Discussion

Excitation Spectra and Identification of the Carrier. Figure 2 shows the LIF excitation and R2C2PI spectra observed from an indene/argon discharge. The dominant feature observed in the LIF spectrum coincides with that seen by R2C2PI of $m/z = 117$. The additional band features in the LIF spectrum not observed by R2C2PI of $m/z = 117$ have been determined to be carried by the 1-phenylpropargyl radical at $m/z = 115$ (1PPR, Figure 1),[11] and an unidentified species carrying $m/z = 133$ (analytical mass spectroscopy has revealed a mass 134 impurity in the indene sample that is likely to be the progenitor of the 133 radical spectrum). R2C2PI spectra observed on the mass channels $m/z = 115$ and 133 are also presented in Figure 2. The strongest band in the LIF and the R2C2PI $m/z = 117$ spectra at 21159 cm^{-1} is determined to be the origin band of the $m/z = 117$ species since no further excitation features were observed to the red.

The photoionization efficiency (PIE) curve of the species carrying $m/z = 117$ is shown in Figure 3. The ionization potential (IP) of the spectral carrier was determined to be 6.578 ± 0.001 eV. From the PIE curve, it may be seen that this error is conservative.

In order to identify the spectral carrier with $m/z = 117$, we changed the precursor molecule and observed the effect on

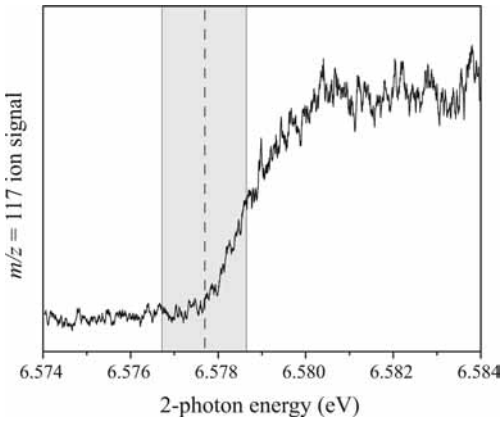

Figure 3. The photoionization efficiency curve of the 1-indanyl radical. A conservative confidence interval of ± 0.001 eV is shaded.

signal. First, allyl benzene ($C_6H_5-CH_2CHCH_2$), an isomer of indane, was utilized and no 2-color resonant ion signal on the $m/z = 117$ channel was observed. Therefore, we ruled out radicals with the monosubstituted benzene skeleton. Using indan (Figure 1) as a precursor increased the resonant $m/z = 117$ signal 3-fold. Since in our experience hydrogen loss is usually effected efficiently in a discharge environment, either the 1-indanyl or 2-indanyl radical is thus considered the most likely carrier of $m/z = 117$. Indeed, the observed excitation spectrum has similar structure to the spectrum of 1-indanyl in a glassy matrix. The matrix spectrum shows a very strong origin at ~20800 cm^{-1} with some weaker features ~1000 cm^{-1} to the blue.[19] However, we could not rule out the possibility of rupture of the five-membered ring, forming radicals with the disubstituted benzene skeleton, and therefore we carried out some quantum chemical calculations of other candidates.

Quantum Chemical Calculations. Density functional theory (DFT) using the B3LYP functional[22,23] was employed to evaluate the relative energies of various isomers of C_9H_9 and their ionization potentials. The results of these calculations are summarized in Table 1. All isomers were found to have singlet cation ground states, except isomers *F* and *G* for which the triplet was calculated to be lower in energy. Calculations were performed with the Gaussian 03[24] package using the 6-311++G(d,p) basis. Geometry optimization and a subsequent vibrational frequency calculation for each isomer was carried out to determine electronic energies with zero-point corrections. Our relative energies of the 1- and 2-indanyl radicals match those of Vereecken et al., who also employed the B3LYP functional with a slightly smaller basis,[10] to the precision reported. The vertical IP of each isomer was obtained by calculation of the energy of the (singlet or triplet) cation at the optimized geometry of the neutral molecule.

As can be seen, the calculated IP of 1-indanyl at 6.53 eV compares well with the experimental value of 6.58 eV. Isomers *B*, *C*, *D*, *F*, and *G* (and in particular *B*, 2-indanyl) are discounted as potential carriers as their calculated IPs are significantly higher than observed. Isomer *E*, which shows a similar calculated IP, is less likely to form due to its higher relative energy. The matching IP and low relative energy demonstrate that the 1-indanyl radical (isomer *A*) is the most likely candidate to carry the spectrum recorded on the $m/z = 117$ channel. Another important piece of experimental information on the radical is the electronic transition energy and fluorescence lifetime. The origin band position of the radical is similar to that of the $\tilde{A}-\tilde{X}$ transitions of the benzyl radical ($T_0 = 22000$ cm^{-1}) and benzylic radicals in general.[25] The fluorescence decay

TABLE 1: Energies and Vertical IPs of Possible Isomers Carrying $m/z = 117$ Obtained by DFT (B3LYP/6-311++G(d,p))

structure	label	ΔE (kJ mol^{-1})	IP[a] (eV)
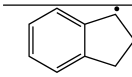	*A*	0	6.53
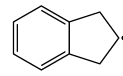	*B*	42	7.46
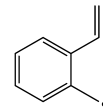	*C*	60	6.98
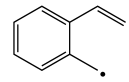	*D*	66	6.95
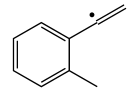	*E*	99	6.58
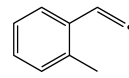	*F*	148	8.18
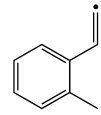	*G*	151	8.13

[a] vertical

profile of the radical observed by pumping the origin band revealed an approximate lifetime of being ~1 μs. This value is comparable to those observed in the visible bands of the benzyl radical.[25] Indeed, the long lifetime is due to the accidentally forbidden nature of the transition whereby there is interference between the transition moments due to the highest occupied molecular orbital (HOMO)−lowest unoccupied molecular orbital (LUMO) and second-highest occupied molecular orbital (SHOMO)−HOMO transitions. These experiments indicate that the electronic structure of the $m/z = 117$ radical is similar to that of a benzylic radical. The assignment of the observed spectrum to the 1-indanyl radical is consistent with these observations and is confirmed below by comparison between an experimental and simulated dispersed fluorescence spectrum.

Dispersed Fluorescence (DF) Spectroscopy and Assignment of the Ground-State Vibrations. Fluorescence from the vibrationless level of the excited state of the radical was dispersed in order to determine the ground state vibrational frequencies. Figure 4 shows the observed DF spectrum. The spectrum shows a very intense origin feature followed by weaker emission features indicating a small geometry change upon electronic excitation.

Vibrational assignment based only on the ground-state frequencies becomes difficult when a large number of vibrational modes exist in a molecule, which may in turn lead to an even larger number of possible combinations of vibrations. In order to assist in the vibrational assignment of the observed spectrum, we calculated the Franck−Condon factors (FCFs) for the emission spectrum. The procedure of the calculation was similar to that described by Sharp and Rosenstock,[26] the only difference being that in the present calculation we used Cartesian coordinates fixed on each atom instead of internal coordinates. Evaluation of the multidimensional Franck−Condon overlap integrals was achieved by recursion relations derived by

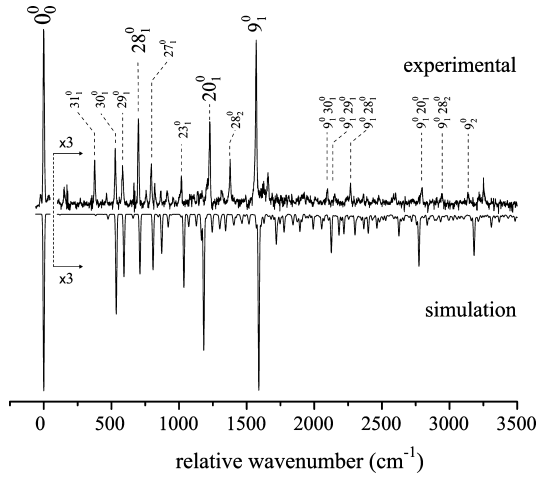

Figure 4. The dispersed fluorescence observed by pumping the 21159 cm^{-1} origin band (top) and the simulated spectrum (bottom).

Ruhoff.[27] The excited state geometries, normal mode of vibration, and harmonic frequencies were obtained with the CASSCF/6-311++G(d,p) level of theory using the MOLPRO package.[28] Nine electrons were seeded into nine orbitals in the CASSCF calculation. The Duschinsky rotation matrix, **J**, and displacement vector, **K**, which are required for the FCF calculation, were computed from the results of the CASSCF and B3LYP calculations for the excited and ground states respectively.

The simulated spectrum from the result of the FCF calculation is shown in Figure 4. The intensity factor used in the simulation, **FCF** $\times \Delta\tilde{\nu}^3$, enables direct comparison with the experimental spectrum. Vibrational assignment of the observed DF spectrum was therefore achieved by comparison with the simulation spectrum. Most of the medium intensity peaks were reproduced in the calculated spectrum and therefore assignments we were able to made for them. The present assignments are listed in Table 2 and those for some of the intense bands are explicitly indicated in Figure 4. The FC active modes are ν_9, ν_{20}, ν_{23}, and ν_{27-31}. These modes all involve in-plane distortion and breathing of both the benzene and five-membered ring systems.

As indicated in Table 2, the lowest nine modes of a' symmetry are all well matched between experiment and theory. Indeed, a scaling of the calculated frequencies by 0.975 would improve the match further. It is significant that there is no serious discrepancy between experiment and calculation up to 1000 cm^{-1}, and the lowest frequency modes are extremely well calculated, as observed for other radicals of a similar nature.[11] The discrepancy for ν_{20} comes from the method of assignment. Rather than relying on frequency matching, the modes were assigned by Franck−Condon factor guided by the CASSCF and DFT calculations. The large number of modes around 1200 cm^{-1} makes the character of the calculated modes very sensitive to the potential energy surface. As such, small errors in the PES could lead to large errors in the modes' character and thus erroneous FCF and assignment.

A similar FCF calculation of the excitation spectrum poorly reproduced the experimental spectrum and as such no reliable assignments were made for the excited state. This is probably due to some significant errors in the CASSCF frequencies and normal modes used for the excited state in the FCF calculation, though the good agreement for the dispersed fluorescence indicates that the CASSCF geometry is probably reliable. A rigorous assignment of the excitation spectrum of the 1-indanyl radical warrants further investigation. However, despite this minor setback the spectroscopic evidence presented here provides a positive identification of the vacuum-isolated 1-indanyl radical for the first time.

TABLE 2: Ground-State Vibrational Frequencies and Assignments of the 1-Indanyl Radical Observed in the DF Spectrum[a]

frequency	calc[b]	assignment
0	0	0_0^0
377	384	31_1^0
529	536	30_1^0
583	593	29_1^0
700	711	28_1^0
757		(31_2^0)
794	808	27_1^0
821	872	(26_1^0)
865	920	(25_1^0)
1006	1016	(24_1^0)
1018	1036	23_1^0
1211	1166	(21_1^0)
1228	1183	20_1^0
1378		28_2^0
1570	1590	9_1^0
2096		$9_1^0 30_1^0$
2151		$9_1^0 29_1^0$
2267		$9_1^0 28_1^0$
2794		$9_1^0 20_1^0$
2940		$9_1^0 28_2^0$
3137		9_2^0

[a] Assignments have been made by comparison with the simulated dispersed fluorescence spectrum (Figure 4). All frequencies in cm^{-1}. Tentative assignments for weaker bands are given in parentheses. [b] Unscaled B3LYP/6-311++G(d,p).

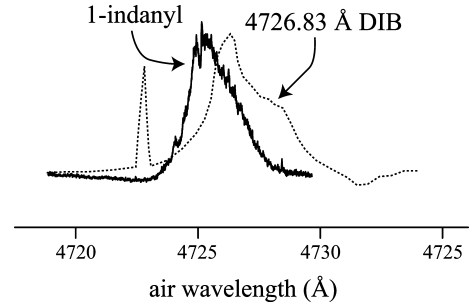

Figure 5. A comparison of the origin band of the 1-indanyl radical to the nearest diffuse interstellar band.[30] The DIB profile, toward HD 204827 has been adapted from ref 30. The 1-indanyl radical cannot be held responsible for the interstellar feature.

Chemical Implications. It has been calculated previously that the 1-indanyl radical represents the global minimum on the C_9H_9 potential energy surface.[10] As such, its observation by laser spectroscopy as an isolated radical is significant as it allows the remote detection of the radical in inaccessible environments such as combustion, or even the interstellar medium. The free 1-indanyl radical does not carry a diffuse interstellar band, as demonstrated in Figure 5, but due to the barrierless reaction of a hydrogen atom with indene, it is likely that if indene moieties are presented by large organic molecules in the interstellar medium then 1-indanyl radical moieties would be formed facilely. It remains to be shown how the 1-indanyl motif might behave spectroscopically in various macromolecular envrionments.

The formation of 1-phenylpropargyl from indene further underlines its likely importance in the chemistry of PAH formation and should be included in future computational modeling of the reaction schemes leading to indene formation. The radical observed at $m/z = 133$ is yet to be identified but is likely a benzylic radical formed through hydrogen abstraction of the 134 amu impurity.

The 1-indanyl species is the most recent in a series of resonance-stabilized radicals produced in hydrocarbon discharges in our group including 1-phenylpropargyl[11] and both isomers of 1-vinylpropargyl.[29] It has become clear that resonance-stabilized radicals are resilient species formed abundantly in our hydrocarbon discharges. Their ubiquity highlights a chemical importance which is yet to be fully appreciated.

Conclusions

Using the complementary LIF and R2C2PI techniques, the excitation spectrum carried by $m/z = 117$ observed in an indene/argon discharge in the region 20800−22600 cm^{-1} has been identified to be due to the 1-indanyl radical. Its ionization potential has been determined to be 6.58 eV, a measurement which will aid its identification by PIE spectroscopy. A DF spectrum observed after pumping the origin band has been recorded, and assignments of the DF spectrum were made with the help quantum chemical calculations. As this radical is the global minimum on the C_9H_9 potential energy surface, it is likely to be observed in future studies of hydrocarbon radical chemistry. This study provides the ionization potential and resonant wavelengths necessary to make a positive identification.

Acknowledgment. This research was supported under the Australian Research Council's (ARC) Discovery funding scheme (Project Number DP0985767). T.P.T. acknowledges the University of Sydney for a University Postgraduate Award. N.C. acknowledges the Endeavor International Postgraduate Research Scholarship and the University of Sydney International Scholarship. K.N. acknowledges the ARC for an Australian Research Fellowship. We thank Professor Y. Endo at the University of Tokyo for allowing us access to his computer system for use of the MOLPRO suite of programs.

References and Notes

(1) Melius, C. F.; Colvin, M. E.; Marinov, N. M.; Pitz, W. J.; Senkan, S. M. *Proc. Combust. Inst.* **1996**, 685–692.
(2) Kern, R. D.; Singh, H. J.; Wu, C. H. *Int. J. Chem. Kinet.* **1988**, *20*, 731–747.
(3) McEnally, C. S.; Pfefferle, L. D.; Atakan, B.; Kohse-Höinghaus, K. *Prog. Energ. Combust.* **2006**, *32*, 247–294.
(4) Miller, J. A.; Melius, C. F. *Combust. Flame* **1992**, *91*, 21–39.
(5) Melius, C. F. *Combust. Flame* **1992**, *339*, 365–376.
(6) Miller, J. A.; Klippenstein, S. J. *J. Phys. Chem. A* **2001**, *105*, 7254–7266.
(7) Hoyermann, K.; Mauβ, F.; Zeuch, T. *Phys. Chem. Chem. Phys.* **2004**, *6*, 3824–3835.
(8) Atakana, B.; Lamprecht, A.; Kohse-Höinghaus, K. *Combust. Flame* **2003**, *133*, 431–440.
(9) Richter, H.; Howard, J. B. *Prog. Energy Combust. Sci.* **2000**, *26*, 565–608.
(10) Vereecken, L.; Peeters, J.; Bettinger, H. F.; Kaiser, R. I.; v. R.; Schleyer, P.; Schaefer, H. F. *J. Am. Chem. Soc.* **2002**, *124*, 2781–2789.
(11) Reilly, N. J.; Kokkin, D. L.; Nakajima, M.; Nauta, K.; Kable, S. H.; Schmidt, T. W. *J. Am. Chem. Soc.* **2008**, *130*, 3137–3142.
(12) Désert, F.; Boulanger, F.; Puget, J. *Astron. Astrophys.* **1990**, *237*, 215–236.
(13) Sarre, P. J. *J. Mol. Spectrosc.* **2006**, *238*, 1–10.
(14) Güthe, F.; Ding, H.; Pino, T.; Maier, J. P. *Chem. Phys.* **2001**, *269*, 347–355.
(15) Newby, J. J.; Stearns, J. A.; Liu, C.-P.; Zwier, T. S. *J. Phys. Chem A* **2007**, *111*, 10914–10927.
(16) McVicker, W. H.; Marsh, J. K.; Stewart, A. W. *J. Chem. Soc.* **1924**, *125*, 1743–1750.
(17) Brocklehurst, B.; Robinson, J. S.; Tawn, D. N. *J. Phys. Chem.* **1972**, *76*, 3710–3713.
(18) Brocklehurst, B.; Tawn, D. N. *Spectrochim. Acta* **1974**, *30A*, 1807–1815.
(19) Izumida, T.; Inoue, K.; Noda, S.; Yoshida, H. *Bull. Chem. Soc. Jpn.* **1981**, *54*, 2157–2518.
(20) Deniau, C.; Deroulede, A.; Kieffer, F.; Rigaut, J. *J. Lumin.* **1971**, *3*, 325–350.
(21) Land, E. J. *Prog. React. Kinet.* **1965**, *3*, 369.
(22) Becke, A. D. *J. Chem. Phys.* **1993**, *98*, 5648.
(23) Lee, C.; Yang, W.; Parr, R. G. *Phys. Rev B.* **1988**, *37*, 785.
(24) Frisch, M. J.; Trucks, G. W.; Schlegel, H. B.; Scuseria, G. E.; Robb, M. A.; Cheeseman, J. R.; Montgomery, J. A., Jr.; Vreven, T.; Kudin, K. N.; Burant, J. C.; Millam, J. M.; Iyengar, S. S.; Tomasi, J.; Barone, V.; Mennucci, B.; Cossi, M.; Scalmani, G.; Rega, N.; Petersson, G. A.; Nakatsuji, H.; Hada, M.; Ehara, M.; Toyota, K.; Fukuda, R.; Hasegawa, J.; Ishida, M.; Nakajima, T.; Honda, Y.; Kitao, O.; Nakai, H.; Klene, M.; Li, X.; Knox, J. E.; Hratchian, H. P.; Cross, J. B.; Bakken, V.; Adamo, C.; Jaramillo, J.; Gomperts, R.; Stratmann, R. E.; Yazyev, O.; Austin, A. J.; Cammi, R.; Pomelli, C.; Ochterski, J. W.; Ayala, P. Y.; Morokuma, K.; Voth, G. A.; Salvador, P.; Dannenberg, J. J.; Zakrzewski, V. G.; Dapprich, S.; Daniels, A. D.; Strain, M. C.; Farkas, O.; Malick, D. K.; Rabuck, A. D.; Raghavachari, K.; Foresman, J. B.; Ortiz, J. V.; Cui, Q.; Baboul, A. G.; Clifford, S.; Cioslowski, J.; Stefanov, B. B.; Liu, G.; Liashenko, A.; Piskorz, P.; Komaromi, I.; Martin, R. L.; Fox, D. J.; Keith, T.; Al-Laham, M. A.; Peng, C. Y.; Nanayakkara, A.; Challacombe, M.; Gill, P. M. W.; Johnson, B.; Chen, W.; Wong, M. W.; Gonzalez, C.; Pople, J. A. *Gaussian 03*, rev. C.02; Gaussian, Inc.: Wallingford, CT, 2004.
(25) Fukushima, M.; Obi, K. *J. Chem. Phys.* **1990**, *93*, 8488–8497.
(26) Sharp, T. E.; Rosenstock, H. M. *J. Chem. Phys.* **1964**, *41*, 3453–3463.
(27) Ruhoff, P. T. *Chem. Phys.* **1994**, *186*, 355–374.
(28) Werner, H.-J., et al. *MOLPRO*, version 2008.1, a package of ab initio programs, 2008.
(29) Reilly, N. J.; Nakajima, M.; Troy, T. P.; Chalyavi, N.; Duncan, K. A.; Nauta, K.; Kable, S. H.; Schmidt, T. W. *J. Am. Chem. Soc*., in press.
(30) Hobbs, L. M.; York, D. G.; Snow, T. P.; Oka, T.; Thorburn, J. A.; Bishof, M.; Friedman, S. D.; McCall, B. J.; Rachford, B.; Sonnentrucker, P.; Welty, D. E. *Astrophys. J.* **2008**, *680*, 1256–1270.

JP905831M